Catal Lett (2008) 121:151–157
DOI 10.1007/s10562-007-9312-5

Sol–gel Preparation of K–Co–Mo Catalyst and its Application in Mixed Alcohol Synthesis from CO Hydrogenation

Jun Bao · Yi-Lu Fu · Guo-Zhu Bian

Received: 29 June 2007 / Accepted: 15 October 2007 / Published online: 27 October 2007

Abstract A kind of K–Co–Mo catalyst with large surface area, small particle size and homogenous components distribution was prepared by sol–gel method using citric acid as complexant, and characterized by XRD, BET, HR-TEM, EXAFS and TPD techniques. The activity for mixed alcohol synthesis from syngas on the catalysts was investigated. During the preparation, a gelation process was adopted to prevent the components from precipitating during the solvent extraction and keep the homogeneity and small particle size of final products. Heat-treated the dried gel in argon, the decomposition of critic acid partly reduced the sample and decreases the particle sizes remarkably. The synthesized K–Co–Mo catalyst exhibited excellent performance for mixed alcohol synthesis from CO hydrogenation, which may be due to its large surface area and small particle size creating more active sites. Beside it, the homogeneity of various components was also helpful to enhance the synergistic effect of Co promoters. The high selectivity to the $C_{2+}OH$ was due to the large amount of SH species adsorbed on the catalyst surface.

Keywords Sol–gel method · K–Co–Mo catalyst · Mixed alcohol synthesis · CO hydrogenation

1 Introduction

The catalytic conversion of syngas to mixed alcohol is a potential route for providing clean fuels and chemical feedstock. The most promising application of the mixed alcohol is as an additive for gasoline to increase the octane number and hopeful to replace the MTBE (methyl *tert*-buthyl ether) to reduce the environmental pollution [1, 2]. Several types of catalysts were developed for the reaction [3, 4], therein alkali-promoted molybdenum catalysts are more attractive for potential commercial aspects because of their high catalytic activity, excellent sulfur-tolerance and coke-built tolerance [5–7].

The activity and selectivity for mixed alcohol synthesis over Mo-based catalysts are significantly affected by the Mo species structures, the additives and reaction conditions. Jiang et al. [8] have studied the structure of sulfided K–Mo/Al_2O_3 catalysts, and found that the decrease of particle size of MoS_2 was in favorable to H_2 absorption and improved the selectivity for C_{2+} alcohol. Li et al. [9] have reported that improving the dispersion of sulfided Mo species could enhance the alcohol activity. They suggested that decreasing the size of Mo species would create more active sites, such as coordinately unsaturated molybdenum sites (Mo(CUS)), to improve the properties of alcohol synthesis.

It was found that 3d transition metals, such as cobalt or nickel, are effective promoters of the Mo-based catalysts for enhancing the alcohol production, especially for improving the C_{2+} alcohol selectivity [10–12]. Tatsumi et al. [10] studied the catalytic performance and structure of reduced K–Ni–Mo/SiO_2, and suggested that Ni-Mo alloy was the active species for alcohol formation. Bian et al. [12] found that for sulfided K–Co–Mo/Al_2O_3 catalysts, enhancing the interaction between Co and Mo atoms

---

J. Bao (✉)
National Synchrotron Radiation Laboratory, University of Science and Technology of China, Hefei 230026, P.R. China
e-mail: baoj@ustc.edu.cn

Y.-L. Fu · G.-Z. Bian
Department of Chemical Physics, University of Science and Technology of China, Hefei 230026, P.R. China

improved the activity and selectivity for mixed alcohol remarkably.

The above results indicated that for Mo-base catalysts, decreasing the size of Mo species or enhancing the interaction between promoter and Mo may be the effective ways for improving the alcohol formation. However these reported catalysts were prepared generally by two classical methods: the impregnation technique and the precipitation method. These conventional methods do not always produce homogenous distributions of various components, and the effect of promoters is not exerted adequately. Calcinations at high temperature can obtain the multi-components catalysts, but result in large particles and small BET surface area. This obviously limits the activity of the catalysts. Yoshimura et al. [13] have reported the preparation of Co–Mo/Al_2O_3 with citric acid as a ligand, in which the catalysts were prepared by the wetness impregnation of γ-Al_2O_3 with aqueous solutions of citric acid containing the Co and Mo components. The synthesized sample exhibited an increase in the HDS activity due to the decrease in the lateral size of MoS_2-like crystallites. In this study, a novel K–Co–Mo catalyst with large surface area and homogenous component distribution was prepared by a modified sol–gel technique using citric acid as a complexant. The structures and catalytic performances for mixed alcohol synthesis were investigated.

2 Experimental

2.1 Catalysts Preparation

The K–Co–Mo particles with Co/Mo molar ratio = 1 and K/Mo = 0.4 were prepared by a sol–gel method using citric acid as a complexing hydroxy acid. A typical procedure is as follows: firstly the $Co(NO_3)_2 \cdot 6H_2O$ (AR.) solution (3.989 g in 15 ml distilled water) and $(NH_4)_6Mo_7O_{24} \cdot 6H_2O$ (AR.) solution (2.42 g in 20 ml distilled water) were mixed. With addition of drops of NH_4OH, a purple precipitate was formed in the solution. Then a certain amount of citric acid (AR.) solution was added into the mixed solution under constant stirring and dissolved the precipitate. Finally the K_2CO_3 solution (0.379 g in 5 ml distilled water) was dropped slowly into the solution and no new precipitation was formed. The pH value of the mixed solution was adjusted by addition of HCOOH or NH_4OH. The solution was kept in a water bath at 338 K for about 6 h until the solution became a gel with high viscosity. During the gelation process, the solution kept homogeneous and no precipitate was formed. The as-prepared gel was dried at 393 K for 15 h and calcined in argon or air at 673 K for 4 h.

For comparison, an additional K–Co–Mo sample with the same composition was prepared by the conventional impregnation method as report in literature [14].

The mixture of CS_2/H_2, used as sulfiding gas, was obtained by passing H_2 through 273 K CS_2 liquid. The sulfided samples were obtained by sulfiding the oxidized samples in a flow (30 ml/min) of CS_2/H_2 at 673 K for 6 h.

2.2 Catalysts Characterization

Surface area was determined by using the BET method in an ASAP-2000 instrument, employing N_2 as the adsorbate.

X-ray diffraction (XRD) patterns were measured in a D/MAX-γA rotatory target diffractometer with Cu Kα radiation (λ_a = 0.15418 nm).

The high-resolution transmission electron microscopy (HR-TEM) analysis was carried out using a JEOL 2010 microscope, with a line resolution of approximately 0.14 nm.

The H_2 temperature-programmed desorption (TPD) of sulfided samples was performed on a chromatographic system. The sample (0.1 g) was first treated in a flow of argon (nominal purity 99.99%) at 673 K for 2 h and cooled to 573 K, and then H_2 adsorption for 1 h. The sample saturated with adsorbed H_2 was cooled to 373 K in a flow of H_2 (20 ml/min), and stood at this temperature in a flow of argon until the base line of the gas chromatograph remained constant. Then it was subjected to temperature programmed desorption of H_2 at a heating rate of 10 K/min.

The Mo K-edge spectra of extended X-ray absorption fine structure (EXAFS) were measured on the beam-line of 4WIB of Beijing Synchrotron Radiation Facility (BSRF). The storage ring was operated at 2.2 GeV with a typical current of 50 mA. The fixed-exit Si(111) flat double crystals were used as a monochromator. All samples were ground and sieved through 400 meshes. The EXAFS data analysis was performed following a standard procedure [15].

2.3 Catalytic Reaction Measurement

The catalytic performance of sulfided K–Co–Mo catalysts for mixed alcohol synthesis was measured using a fixed-bed reactor equipped with an on-line gas chromatograph. For each experiment, 0.5 g of the sample was charged into a stainless steel reactor with an inner diameter of 6 mm. The syngas is composed of CO (30%), H_2 (60%), and N_2 (10%). The effluent gas was cooled to 273 K and separated into gas and liquid phases at high pressure. The gaseous products were directly analyzed on a chromatograph through a sampling valve, and liquid one was collected for a proper period. The volume and weight were measured and subsequently analyzed on the same chromatograph by injection. The contents of CO and CO_2 in the gas phase and H_2O contents in liquid products were analyzed on a 2 m TDX-01 column by using a thermal conductivity detector (TCD). Argon was used as a carrier gas. The hydrocarbons, alcohol and other oxygenated compounds were analyzed on a 2 m Porapak Q column by using a flame ionization detector (FID) with N_2 as carrier gas. The composition of hydrocarbons was calculated using 1.04% CH_4 as standard gas, while that of the mixed alcohol was calculated directly from the peak areas by using a standard liquid of mixed alcohol.

3 Results and Discussion

3.1 XRD and BET Results

During the preparation process, the purple precipitate formed in the mixed solution with addition of a little NH_4OH was Co–Mo compound oxides. The addition of citric acid dissolved the precipitate and formed a homogeneous solution because the organic ligand has a strong complexing capability to the Mo(IV) ions, which promoted the decomposition of Co–Mo precipitate. The purpose of gelation is to prevent the components from precipitating during the solvent extraction and keep the homogeneity and small particle size of final products. In the process, the pH value and amount of citric acid play an important role. The appropriate conditions are pH 3.5 and L/M = 0.4 (L/M: the molar ratio of citric acid to metallic ions) for preparing the well-dispersed particles [16]. Actually, under the condition of pH 3.5 and L/M = 0.4–0.8, the solution can keep homogeneous and no precipitate was formed during the gelation. However the excessive citric acid is unfavorable because it will release a lot of heat during the calcinations and result in the increase of particles size.

For clarify, the samples prepared by sol–gel method under conditions of pH 3.5 and L/M = 0.4 and calcined in argon and air were denoted as KCM01 and KCM02 respectively, the one prepared by conventional method was denoted as KCM03. Accordingly, the sulfided samples were denoted as SKCM01, SKCM02 and SKCM03 respectively.

Figure 1 shows the XRD patterns of oxidized samples, they indicated several phases as expected. For KCM03 sample, the strong peaks can be assigned to $CoMoO_4$ (d = 0.337, 0.327, 0.383, 0.267, 0.315, 0.232, 0.193, 0.277, 0.468, 0.286, 0.227, 0.175, 0.203 nm), CoO (d = 0.209, 0.245, 0.151 nm) and several K–Mo–O species, such as $K_2Mo_3O_{10}$ (d = 0.327, 0.350, 0.690 nm), $K_2Mo_4O_{13}$ (d = 0.350, 0.298, 0.286, 0.690, 0.267, 0.315, 0.468, 0.383, 0.327, 0.232, 0.203, 0.277 nm) and $K_{0.3}MoO_3$ (d = 0.818, 0.315 nm). Besides, the Co_3O_4 phase (d = 0.245, 0.286, 0.203, 0.468 nm) may also exist on the sample.

The diffraction peaks of KCM02 were similar to that of KCM03, but the intensities are much lower, indicating a smaller crystallite sizes.

It is interesting to note that the XRD patterns of KCM01 were quite different from those of KCM02 and KCM03. Only very weak broad peaks were detected on the sample. The d-values of 0.337, 0.267, 0.315, 0.286, 0.175 nm were assigned to $CoMoO_4$. The other peaks (d = 0.250, 0.243, 0.492, 0.350, 0.205, 0.199, 0.163, 0.154 nm) can be assigned to $CoMoO_3$, a low-valence phase. These results suggested that the decomposition of citric acid in argon partly reduced the sample and decreased the crystallite size remarkably.

The XRD results of sulfided K–Co–Mo samples are presented in Fig. 2. After sulfidation, the diffraction peaks observed in the oxidized samples completely disappeared. In the meantime, Co_9S_8 (d = 0.299, 0.287, 0.176, 0.192 nm) and MoS_2 species (d = 0.618, 0.274, 0.228, 0.158 nm) appeared. Besides, the $CoMoS_{3.13}$ species (d = 0.618, 0.274, 0.228, 0.192, 0.158 nm) may also exist. The diffraction intensities decreased in the order of SKCM03 > SKCM02 > SKCM01. For comparison purpose, the XRD pattern of supported K–Co–Mo/C sulfided catalysts (prepared by impregnation technique, see [17]) was also listed. The supported sample showed a similar diffraction pattern to the three present catalysts and its diffraction intensities was almost the same as that of the SKCM01, which indicated that after sulfidation, the sol–gel derived sample still kept a small size.

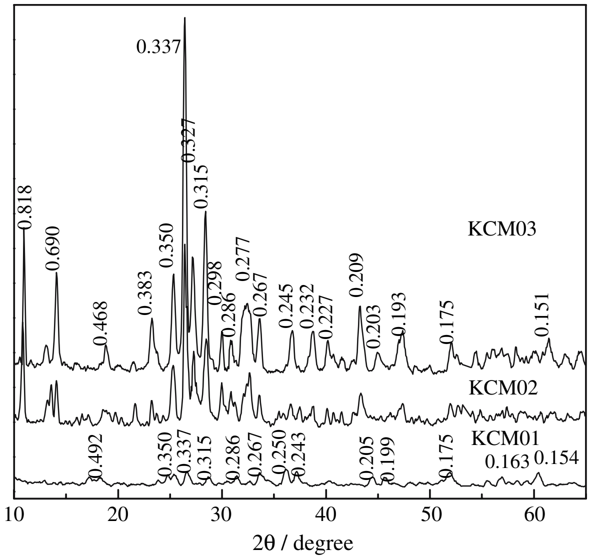

Fig. 1 XRD patterns of oxidized K–Co–Mo samples

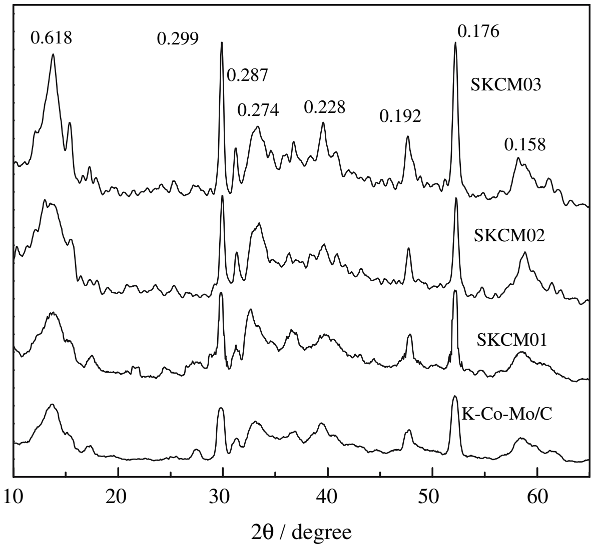

Fig. 2 XRD patterns of sulfided K–Co–Mo samples

The BET surface areas of oxidized and sulfided samples are presented in Table 1. As expected, the particles prepared by sol–gel method had much larger surface area, especially the one heat-treated in argon.

3.2 HR-TEM Result

The microstructures of the three oxidized samples were investigated using the HR-TEM. As shown in Fig. 3, the KCM01 sample showed a high homogeneity and the amorphous char was clearly observed. The EDS analysis demonstrated that besides the K, Co, Mo, O, the element C also existed in the sample. The formation of amorphous char was attributed to the decomposition of citric acid in argon. The size of K–Co–Mo active particles in the sample was estimated about 2–5 nm, and they were homogeneously dispersed in the amorphous char. For the KCM02 that heat-treated in air, the particles had spherical shapes with size of ~25 nm, and no char was observed. The KCM03 sample derived from impregnation method showed irregular shapes and their particle sizes were more than 500 nm. The results clearly indicated that the sol–gel synthesized K–Co–Mo catalyst had smaller particle size and homogenous components distribution. The heat-treatment of dried gel in argon can decrease the particle size significantly.

3.3 EXAFS Result

The magnitude of the Fourier Transforms (FT) of $k^3 \times (k)$ ($\Delta k = 19.0$–$128.0\ \mathrm{nm}^{-1}$) of Mo K-edge EXAFS spectra of the sulfided K–Co–Mo samples together with the MoS_2 standard compound are shown in Fig. 4. The structure parameters of Mo atoms in the samples were calculated and listed in Table 2. MoS_2 is of hexagon structure with one molybdenum atom is surrounded by six sulfur atoms at a distance of 0.241 nm and six molybdenum neighbors at 0.316 nm. As shown in Fig. 4, for the three samples, two prominent peaks corresponding to the nearest Mo–S and Mo–Mo shell were observed at about 0.200 and 0.280 nm. They located almost at the same positions as those of the MoS_2, indicating that the molybdenum in the sulfided samples mainly existed in the form of MoS_2-like species. No clear indication of Mo–Co coordination ($R_{\mathrm{Mo–Co}}$ = 0.28 nm) were observed in Mo K-edge EXAFS spectra. This might be due to the fact that for the catalysts the Mo–Co coordination number was low and overlapped by the strong Mo–Mo coordination shell since the near coordination distance [17].

From Table 2, the Mo–S and Mo–Mo coordination numbers of the three catalysts, especially the latter, were clearly lower than those of bulk MoS_2. It indicated that the MoS_2-like species in sulfided samples were small particles. Comparing the three samples, both Mo–S and Mo–Mo coordination numbers decreased in the following order: SKCM03 > SKCM02 > SKCM01, indicating that the MoS_2-like species in the sample prepared by sol–gel method had smaller crystallite sizes, consistent with the XRD result.

3.4 H_2 TPD Result

Figure 5 shows the H_2 TPD patterns of the sulfided samples. For the three samples, one desorption peak at temperatures between 300 and 500 °C was observed, consistent with the previous TPD results obtained in our laboratory [8, 18]. Besides, a more intensified desorption peak was also observed between 550 and 800 °C. The areas of both desorption peaks, especially the latter, increased in the order of SKCM03 < SKCM02 < SKCM01.

At temperature of 300 °C, the absorbed H_2 molecules possibly dissociate on the Mo(CUS) sites, and then by spillover or other ways, migrate to the basal plane of MoS_2

Table 1 The BET surface area of the oxidized and sulfided samples

Sample	Oxidized sample			Sulfided sample		
	KCM01	KCM02	KCM03	SKCM01	SKCM02	SKCM03
S_{BET} ($m^2\ g^{-1}$)	56.8	35.5	5.6	49.7	30.5	11.3

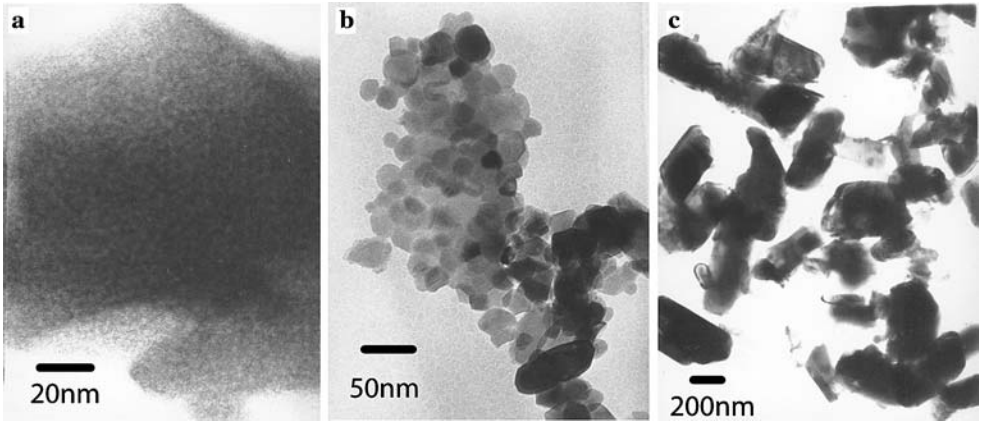

Fig. 3 The HR-TEM images of sample KCM01 (**a**), KCM02 (**b**) and KCM03 (**c**)

species, where it bonds with sulfur atoms and remains as SH species [19, 20]. In view of the mechanism of H_2 adsorption on the molybdenum sulfides, the two desorption species revealed in H_2 TPD for the sulfided samples can be ascribed to the desorption of the dissociated hydrogen on Mo(CUS) sites (300–500 °C) and H_2S (>500 °C) relating to the surface SH species, as recognized by some authors [8, 18, 21]. The increase in the amount of both desorption species indicated that the SKCM01 and SKCM02 catalysts adsorbed much more amount of H species, especially the SH species on the surface than those of the SKCM03.

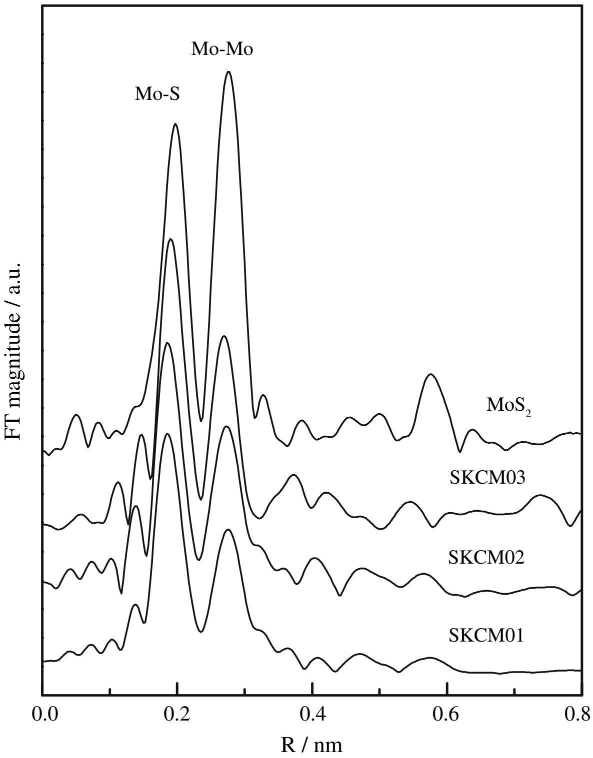

Fig. 4 Fourier transforms of Mo K-edge EXAFS spectra of MoS_2 and the sulfided K–Co–Mo samples

3.5 Catalytic Activity

The catalytic performances of the K–Co–Mo sulfided catalysts for mixed alcohol synthesis were tested at $H_2/CO = 2$, 583 K, 5.0 MPa and GHSV = 4,800 h^{-1}. The measured stable activity, selectivity and $C_1OH/C_{2+}OH$ ratio after reaction for 24 h are shown in Table 3. For comparison purpose, the reaction results of K–MoS_2 tested under same condition were also listed in the table. Over the un-promoted K–MoS_2 sample, the activity and selectivity toward alcohol synthesis were rather low, and the predominant products were hydrocarbons. When the cobalt was incorporated, the space-time-yield (STY) of the total alcohol and the selectivity for C_{2+} alcohol remarkably increased, indicating that the presence of cobalt in the catalysts was much effective for alcohol formation, consistent with the previous reports [10–12]. Comparing the three K–Co–Mo samples, the catalysts SKCM01 and SKCM02 that prepared by sol–gel method exhibited much

Table 2 Structure parameters of Mo–S and Mo–Mo coordination for MoS_2 and the sulfided samples

Sample	Bond	R (nm)	N	$\Delta\sigma^2$ (10^{-6}/nm)[a]	ΔE_0 (eV)[b]
MoS_2	Mo–S	0.241	6.0		
	Mo–Mo	0.316	6.0		
SKCM01	Mo–S	0.239	4.0	8	–1.30
	Mo–Mo	0.317	2.1	12	0.73
SKCM02	Mo–S	0.240	4.6	7	1.08
	Mo–Mo	0.316	2.6	6	–1.42
SKCM03	Mo–S	0.241	5.4	3	0.58
	Mo–Mo	0.316	3.3	5	1.66

[a] Relative Debye–Waller factor of the sample to that of the standard compounds

[b] Correction of the inner potentials of the samples based upon those of the crystalline MoS_2

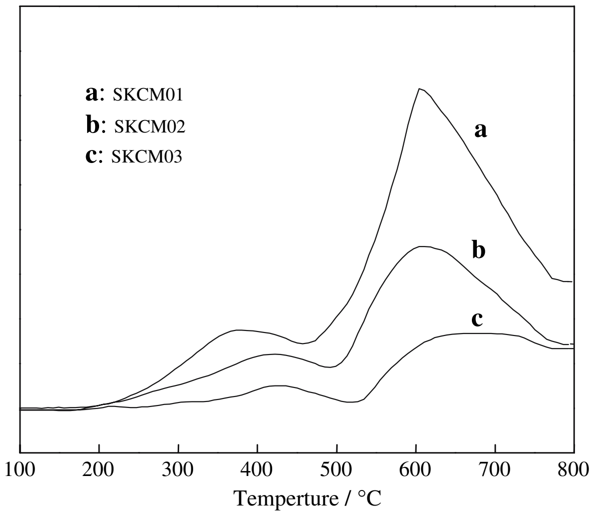

Fig. 5 H_2 TPD patterns of the sulfided K–Co–Mo samples

higher STY of alcohol and selectivity for C_{2+} alcohol than those of SKCM03. Especially over the SKCM01, the alcohol STY was almost two times as high as that of SKCM03.

It is necessary to make a comparison of the presented catalysts with those of previous catalytic systems. Table 4 lists the catalytic performance of SKCM01 and those of some similar catalysts in previous reports [12, 17, 22]. Comparison with the unsupported K–Co–Mo catalysts in patents, the SKCM01 exhibited better activity for alcohol synthesis except that the $C_1OH/C_{2+}OH$ ratio was a little high. It should be mentioned that in the activity measurement of K–Co–Mo catalysts in patents, about 50 ppm of H_2S was presented in the feed gas. It is well known that the addition of H_2S in the synthesis gas can remarkably increase the $C_{2+}OH$ content [23, 24]. For example, on the sulfided K–Mo/C, the $C_1OH/C_{2+}OH$ ratio decreased from 3.69 to 1.03 by adding 110 ppm of H_2S in the feed gas under the condition of 573 K, 20.79 MPa [24]. If operated at appropriate condition, the presented SKCM01 catalyst is expected to have better performance. Supported Mo catalysts generally exhibit better activity for alcohol synthesis than those of the unsupported catalysts [25]. Comparing with the supported K–Co–Mo/Al_2O_3 and K–Co–Mo/C catalysts, it can be seen that the SKCM01 catalyst also showed much higher alcohol activity and selectivity under the same reaction conditions.

The Mo-based catalysts for mixed alcohol synthesis have been widely investigated. The lower oxidation state of Mo, such as metallic Mo and Mo^{4+} is more active for the alcohol formation [26, 27]. In addition, the dispersion and surface area of Mo species are the important issues related to the catalytic properties. Many authors reported that the catalytic active sites on sulfided Mo-based catalysts are due to the so-called coordinately unsaturated molybdenum sites (Mo(CUS)), on which chemisorption of probe molecules can occur [28, 29]. The decrease of size of Mo species can facilitate the H_2 adsorption and migration to form SH species due to creating more Mo(CUS) [8, 9]. Jalowiechi et al. [29] studied the treatment of sulfided Mo catalysts with H_2 and revealed that the supported MoS_2/Al_2O_3 catalysts can store much more amount of H_2 than the unsupported MoS_2 catalysts since the Mo species can be highly dispersed on the support. In light of the above, the

Table 3 Catalytic performance for mixed alcohol synthesis from syngas

Catalysts	CO (C%)	Alc. Sel. (C%)	CH. Sel. (C%)	CO_2 Sel. (C%)	Alc. STY (g/kg h)	C_nOH Sel. (C%)			$MeOH/C_{2+}OH$
						MeOH	EtOH	PrOH	
K–MoS_2	5.2	34.7	45.5	19.8	31.2	19.1	14.0	1.6	1.22
SKCM01	15.3	62.4	11.4	26.2	188.6	30.9	26.9	4.6	0.98
SKCM02	12.5	60.5	16.0	23.5	165.8	31.6	25.1	3.8	1.09
SKCM03	9.3	53.6	18.8	27.6	98.9	29.6	21.5	2.5	1.24

Reaction conditions: T = 583 K, P = 5.0 MPa, GHSV = 4,800 h^{-1}, H_2/CO = 2

Table 4 Catalytic performance comparison of the sol–gel catalyst with those of previous similar systems

Sample	Temp. (K)	Press. (MPa)	GHSV (h^{-1})	H_2/CO molar ratio	H_2S added (ppm)	CO Conv. (C%)	Alc. Sel.[a] (C%)	Alc. STY (g/kg h)	$MeOH/C_{2+}OH$	References
SKCM01	583	5.0	4800	2.0	0	15.3	84.6	188.6	0.98	
SKCM01	583	10.0	1200	1.0	0	61.3	73.2	146.8	0.48	
K–Co–Mo	578	10.45	1300	0.98	50	39.0	75.7	115.0	0.39	[22]
K–Co–Mo/C	603	5.0	4800	2.0	0	14.5	27.4	107.6	0.68	[17]
K–Co–Mo/Al_2O_3	583	5.0	4800	2.0	0	6.83	26.19	29.07	1.05	[12]

[a] Based on a CO_2-free basis

high alcohol activity of the sol–gel catalyst in this study should be attributed to its characteristics of large surface area and homogenous distribution of multi-components. Large specific surface area and small particle size contributed to create more Mo(CUS). The homogeneity of various components was suggested to enhance the synergistic effect of Co promoters [8, 10, 12]. The high $C_{2+}OH$ selectivity over the sol–gel catalyst was due to the large amount of SH species adsorbed on the surface, as revealed by the TPD results.

4 Conclusion

With citric acid as complexant, a novel K–Co–Mo catalyst was prepared by sol–gel method plus a gelation process. Heat-treated the dried gel in argon, the decomposition of citric acid can partly reduce the samples and decrease the particles sizes remarkably. The obtained catalyst had the characteristics of large surface area, small particle size and homogenous components distribution. Compared with the previous similar catalysts, the sol–gel derived catalysts exhibited much better performance for mixed alcohol synthesis from CO hydrogenation. The high selectivity to $C_{2+}OH$ can be attributed to the large amount of SH species absorbed on the catalyst surface.

Acknowledgment The supply of EXAFS experimental facility by Beijing Synchrotron Radiation Facility (BSRF) is gratefully acknowledged.

References

1. Satterfield CN (1991) Heterogeneous catalysis in industrial practice, 2nd edn. McGraw-Hill, New York, p 454
2. Xu X, Doesburg EBM, Scholten JJF (1987) Catal Today 2:125
3. Tronconi E, Rerlazzo N, Pasquon I (1987) Ind Eng Chem Res 26:2122
4. Chaummette P, Courty Ph, Durand D, Grandvallet P, Travers Ch (1984) British Patent 2,158,30
5. Tatsumi T, Muramatsu A, Tominaga H (1984) Chem Lett 685
6. Zhang HB, Yang YQ, Huang HP, Lin CD, Tsai KR (1992) Preprint and abstract book of 10th international congress on catalysis. Busapest, Hungary, 19–24 July 1992, p 253
7. Fu YL, Fujimoto K, Lin PY, Omata K, Yu YS (1995) Appl Catal A 126:273
8. Jiang M, Bian GZ, Fu YL (1994) J Catal 146:144
9. Li ZR, Fu YL, Jiang M (1999) Appl Catal A 187:187
10. Tatsumi T, Muramatsu A, Fukunaga T, Tominaga H (1998) In: Philips MJ, Ternan M (eds) Proceedings of 9th international congress on catalysis, Calgary 1988, vol 2. Chemical Institute of Canada, Ottawa, p 618
11. Fujimoto K, Oba T (1985) Appl Catal 13:289
12. Bian GZ, Fu YL, Ma YS (1999) Catal Today 51:187
13. Yoshimure Y, Matsubayashi N, Sato T, Shimada H, Nishijima A (1991) Appl Catal A 79:145
14. Brito JL, Barbosa AL (1997) J Catal 171:467
15. Sayers DE, Bunker BA (1988) In: Koningsberger DC, Prins CR (eds) X-ray absorption, principles, applications, techniques of EXAFS, SEXAFS and XANES. John Wiley and Sons, Inc., p 211
16. Bao J, Bian GZ, Fu YL (1999) Chin J Catal 20(6):645–648
17. Li ZR, Fu YL, Bao J, Jiang M, Hu TD, Liu T, Xie YN (2001) Appl Catal A 220:21
18. Fu YL, Tang XB, Huang ZG, Fan CZ (1989) Appl Catal A 55:11
19. Wright CJ, Sampson C, Fraser D, Moyes R, Wells PB, Richel C (1980) J Chem Soc Faraday Trans 1 76:1585
20. Wright CJ, Fraser D, Moyes R, Wells PB (1981) Appl Catal 1:49
21. Yerofeyev VI, Kaletchits IV (1984) J Catal 86:55
22. Stevens RR (1989) US Patent 4,882,360
23. Cochran GA, Quarderer GJ (1998) US Patent 4,749,724
24. Conway MM, Murchison CB, Stevens RR (1987) US Patent 4,675,344
25. Li ZR, Fu YL, Jiang M, Hu TD, Liu T, Xie YN (2001) J Catal 199:155
26. Saito M, Anderson RB (1980) J Catal 63:438
27. Tasumi T, Muramatsu A, Tominaga H (1992) Sekiyu Gakkaishi 35(3):233
28. Prins R, De Beer VHJ, Somorjai GA (1989) Catal Rev Sci 31(1&2):1
29. Jalowiecki L, Grimblot J, Bonnelle SP (1990) J Catal 126:101